Robust Control of an Aerial Manipulator Interacting with the Environment

Available online at www.sciencedirect.com

ScienceDirect

IFAC Papers Online CONFERENCE PAPER ARCHIVE

IFAC PapersOnLine 51-13 (2018) 537–542

Robust Control of an Aerial Manipulator Interacting with the Environment ⋆

R. Naldi, A. Macchelli, N. Mimmo, L. Marconi

Department of Electrical, Electronic, and Information Engineering (DEI) "Guglielmo Marconi," University of Bologna, viale del Risorgimento 2, 40136 Bologna, Italy, email: {roberto.naldi, alessandro.macchelli, nicola.mimmo2, lorenzo.marconi}@unibo.it

Abstract: This paper deals with the problem of modelling and controlling a vertical take-off and landing aircraft equipped with a lightweight robotic arm. This system is able to perform complex operations that require the physical interaction with the environment while remaining airborne. Once the dynamical model in the 3D case is provided, a control law able to let the degrees of freedom of the system to track a desired trajectory is derived. The proposed controller takes into account the interaction between the robotic arm and the aerial platform both during free-flight and in the presence of unknown contact forces deriving from the interaction with the environment. The effectiveness and main properties of the proposed control algorithm have been analytically investigated and then demonstrated with the help of an experiment.

Keywords: control of UAVs, robust control, robotics, interaction control, nested saturations

1. INTRODUCTION

Applications in which Unmanned Aerial Vehicles (UAVs) are required to physically interact with the surrounding environment have become a popular research topic in the control and robotic community, see e.g. Mellinger et al. (2013); Marconi et al. (2011); Fumagalli et al. (2012); Lippiello and Ruggiero (2012). In this work, the control of an aerial manipulator that consists of a Vertical Take-Off and Landing (VTOL) airframe, more specifically a ducted-fan configuration (Naldi et al. (2010); Marconi and Naldi (2012)), and a miniature robotic arm is presented.

The control design has been specifically tailored to address the applicative scenario described hereafter. A human operator commands the UAV to reach a constant desired position close to the infrastructure to be inspected, and then performs some inspection-by-contact tasks with the manipulator. The environment is modelled as a vertical compliant surface, which means that reaction forces are applied back to the end-effector and, in turn, to the aerial vehicle during the inspection. To succeed in the task, the control law has to guarantee that the vehicle remains closed to the desired position in presence of the disturbances introduced by the interaction with the vertical surface. To investigate the main dynamical properties of the system, a 3D model is proposed. The model takes into account the 3D dynamics of the UAV, and the manipulator is modeled as an $n = 3$ degrees-of-freedom (d.o.f.) robotic arm with actuated joints. Results have been experimentally validated on a real setup that has been obtained by attaching a lightweight parallel manipulator to a miniature ducted-fan prototype.

Since the UAV is under-actuated, the main challenge is to compensate the coupling forces between the manipulator and the floating base that appear either when the robot moves in free-space, and when the end-effector is in contact situations. With respect to existing contributions in the field, see e.g. Fumagalli et al. (2012); Kobilarov (2014); Lippiello and Ruggiero (2012), uncertainties in the knowledge of the contact forces motivate the adoption of robust control techniques. Then, inspired by classical vectored-thrust control paradigms (Hua et al. (2009); Abdessameud and Tayebi (2010)), a novel control strategy is proposed: the coupling forces are directly taken into account in the definition of the desired force control vector, now obtained by tilting the vehicle in the desired direction and then by applying a certain thrust. This approach naturally leads to a cascade control strategy as in Isidori et al. (2003); Marconi and Naldi (2007) in which the position controller (outer-loop) generates the attitude reference for the inner attitude loop by taking into account, throughout the knowledge of the coupling forces, the interaction with the manipulator and the environment. The stability of the closed-loop system is then investigated using total stability tools for nonlinear control systems (Isidori (1999)). The analysis takes into account the control and mechanical parameters of the system to establish conditions leading to asymptotic or practical tracking of the desired references both in free flight and in the presence of unknown contact forces.

2. NOTATION AND DEFINITIONS

In this paper, let $\mathbb{R}$, $\mathbb{R}_{>0}$, and $\mathbb{R}_{\geq}0$ denote the set of real, positive real and non-negative real numbers, respectively. Given $x \in \mathbb{R}^n$, $|x|$ denotes the Euclidean norm, while, for a function $f : [0, +\infty) \to \mathbb{R}^k$, $k > 0$, define $|f|_\infty = \sup_{t\in[0,\,+\infty)} |f(t)|$, and $|f|_a = \limsup_{t\to+\infty} |f(t)|$. Given

⋆ This work has been partially supported by the European project AirBorne (ICT 780960).

10.1016/j.ifacol.2018.07.335

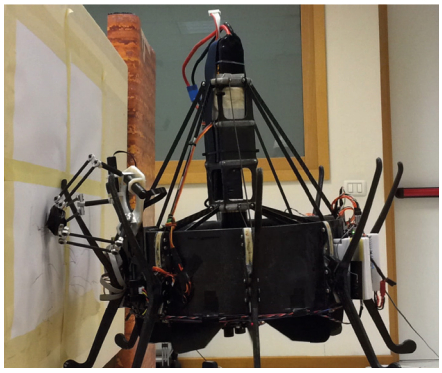

Fig. 1. The aerial manipulator performing a docking manoeuvre.

a class C^n function s, with $n > 0$, $s^{(n)}$ denotes the n-th order derivative.

Here, the notion of Input-to-State Stability (ISS) with restrictions given in (Isidori et al., 2003, Appendix B) is used, and reported below for sake of completeness. Consider a nonlinear system

$$\dot{x}(t) = f\big(x(t), u(t)\big) \tag{1}$$

with state $x \in \mathbb{R}^n$, input $u \in \mathbb{R}^m$, in which $f(0,0) = 0$ and $f(x,u)$ is locally Lipschitz on $\mathbb{R}^n \times \mathbb{R}^m$. Let $\mathcal{X}$ be an open subset of $\mathbb{R}^n$ containing the origin, and let U be a positive number. System (1) is said to be ISS with restriction $\mathcal{X}$ on the initial state $x(0)$ and restriction U on the input $u(\cdot)$ if there exist class-$\mathcal{K}$ functions γ_0 and γ_u such that, for any $x(0) \in \mathcal{X}$ and any input $u \in \mathcal{L}^m_\infty$ satisfying $|u|_\infty \leq U$, the solution $x(t)$ satisfies

- $|x|_\infty \leq \max\{\gamma_0(|x(0)|), \gamma_u(|u|_\infty)\}$,
- $|x|_a \leq \gamma_u(|u|_a)$.

Finally, a *saturation function* is a mapping $\sigma : \mathbb{R}^n \to \mathbb{R}^n$ such that, for $n = 1$

- $|\sigma'(s)| = |{}^{\mathrm{d}\sigma(s)}/_{\mathrm{d}s}| \leq 2$, for all s,
- $s\sigma(s) > 0$, for all $s \neq 0$, $\sigma(0) = 0$,
- $\sigma(s) = \mathrm{sign}(s)$, for $|s| \geq 1$,
- $|s| < |\sigma(s)| < 1$, for $|s| < 1$.

For $n > 1$, the properties listed above are intended to hold component-wise.

3. DYNAMICAL MODEL OF THE AERIAL MANIPULATOR

The prototype considered in this work is the ducted-fan aircraft presented in Naldi and Marconi (2014) equipped with a manipulator (see Fig. 1). The ducted-fan aerial vehicle is a particular configuration of VTOL aircraft in which the propeller is protected by an annular fuselage, denoted as the *duct*. The airframe is composed of two main subsystems. The former consists of a propeller driven by an electric motor and is responsible for producing the thrust force T required to counteract the gravity force. The second subsystem consists of a set of actuated aerodynamic surfaces, denoted as control flaps, acting on the airflow produced by the propeller so as to produce an aerodynamic lift force F and, then, a torque contribution τ that can be employed to govern the attitude of the vehicle.The robotic arm employed in the experiments consists of a parallel Delta configuration, see e.g. Merlet (2000). On the other hand, the theory is developed under the assumption that the manipulator is a generic device with $n = 3$ d.o.f., so that the end-effector can reach a desired position in space with respect to the base of the manipulator itself.

By considering the mechanical layout of the prototype employed in the experiments of Section 5, a number of approximations can be introduced to obtain a model suitable for control design. As far as the manipulator is concerned, by assuming that the mass of the links is negligible compared to the one of the end-effector, denoted by m, the following approximated model is obtained:

$$m\ddot{p}_e = R(\theta)J^{-\mathrm{T}}(q)\tau_q + f_c - mg\hat{e}_3 \tag{2}$$

being $p_e \in \mathbb{R}^3$ the position of the end-effector with respect to the inertial reference frame $(\hat{e}_1, \hat{e}_2, \hat{e}_3)$, with $\hat{e}_3$ along the vertical direction, $q \in \mathbb{R}^3$ the joint coordinates of the manipulator, and $J(q)$ its Jacobian. It is assumed that the manipulator is never in a singular configuration, i.e. that $J(q)$ is always invertible. Note that the inertial position of the end-effector is driven by the control forces τ_q generated by the joint actuators, and it is affected by the force $f_c \in \mathbb{R}^3$ applied by the environment, by the gravity field, being $g \in \mathbb{R}$ the gravity acceleration, and by the attitude θ of the vehicle (e.g., roll, pitch and yaw angles). Consequently, $R(\theta)$ represents the rotation matrix between the reference system $(\hat{e}'_1, \hat{e}'_2, \hat{e}'_3)$ rigidly connected with the UAV, and the inertial reference frame $(\hat{e}_1, \hat{e}_2, \hat{e}_3)$.

The second subsystem is the dynamical model of the UAV that is driven by the thrust T and the torque τ. By assuming that the mass of the manipulator is negligible compared to the one of the vehicle, namely $m \ll M$ (in the experimental set-up, we have that $M \approx 1.8\,\mathrm{kg}$, and $m \approx 0.1\,\mathrm{kg}$), the lateral and longitudinal dynamics can be approximated as

$$M\ddot{p} = -Mg\hat{e}_3 + R(\theta)T\hat{e}'_3 - R(\theta)J^{-\mathrm{T}}(q)\tau_q \tag{3}$$

while, under the hypothesis that the effect of the aerodynamic force can be neglected, the attitude dynamics are governed by

$$\begin{aligned} &\Omega(\theta)\dot{\theta} = \omega \\ &J_{\mathrm{uav}}\dot{\omega} = -\omega \times J_{\mathrm{uav}}\omega + \tau - p'_b \times \left[J^{-\mathrm{T}}(q)\tau_q\right] \end{aligned} \tag{4}$$

where $p \in \mathbb{R}^3$ is the position of the gravity center with respect to $(\hat{e}_1, \hat{e}_2, \hat{e}_3)$, $\omega \in \mathbb{R}^3$ the angular velocity, $\Omega(\theta)$ a linear mapping that depends on the specific representation θ of the UAV attitude, J_{uav} the moment of inertia tensor of the UAV, and $p'_b \in \mathbb{R}^3$ the position of the base of the manipular in the $(\hat{e}'_1, \hat{e}'_2, \hat{e}'_3)$ coordinates. Note that the $\hat{e}'_3$ axis is chosen in the same direction of the thrust T.

The dynamics of the aerial vehicle are affected by the joint generalised torques τ_q governing the manipulator. Moreover, the inertial position of the manipulator is related to the inertial position and orientation of the UAV, and to the joint position of the manipulator via the direct kinematic:

$$p_e = p + R(\theta)\left[p'_b + f_{\mathrm{kin}}(q)\right] \tag{5}$$

Due to this kinematic constraint, the next assumption on the trajectories of the system is necessary.

Assumption 3.1. Denote by $Q \subset \mathbb{R}^3$ the joint workspace of the robotic manipulator. Then, we assume that for the complete system the trajectories evolve in the set

$$\Theta = \left\{(q, p_e, p, \theta) \mid q \in Q,\, p_e, p, \theta \in \mathbb{R}^3 \text{ s.t. (5) holds}\right\} \tag{6}$$

4. CONTROL OF THE AERIAL MANIPULATOR

The inspiring applicative scenario is that the system has to perform inspection-by-contact tasks by means of the manipulator, so the control problem tackled in this paper is to let the end-effector inertial position to track a desired reference trajectory, while the aerial vehicle is maintained at a constant position. As summarised in Assumption 3.1, the reference position of the UAV has to be selected in such a way that the inertial position of the end-effector is within the manipulator operative space. As a main challenge, the control law has to be robust with respect to the presence of possible contacts with the environment, namely when the unknown contact force f_c is applied to the end-effector.

4.1 Robust control of the robotic arm

Given the reference trajectory $p_e^\star(t)$ for the inertial position of the end-effector, consider the following control law

$$\tau_q = J^{\mathrm{T}}(q) R^{\mathrm{T}}(\theta) \left[m \left(\ddot{p}_e^\star + g \hat{e}_3 \right) - \bar{\kappa} \left(\tilde{p}_e, \dot{\tilde{p}}_e \right) \right] \tag{7}$$

in which $\tilde{p}_e = p_e - p_e^\star$ is the position error of the end-effector in the inertial coordinates, and where $\bar{\kappa} : \mathbb{R}^3 \times \mathbb{R}^3 \to \mathbb{R}^3$ is an error feedback controller that is designed by means of the following nested saturation control law:

$$\bar{\kappa} \left(\tilde{p}_e, \dot{\tilde{p}}_e \right) = \; = \bar{\lambda}_2 \sigma \left(\frac{\bar{k}_2}{\bar{\lambda}_2} \left(\dot{\tilde{p}}_e + \bar{\lambda}_1 \sigma \left(\frac{\bar{k}_1}{\bar{\lambda}_1} \tilde{p}_e \right) \right) \right) \tag{8}$$

in which, by following (Isidori et al., 2003, Appendix B), the parameters $\bar{k}_1$, $\bar{k}_2$, $\bar{\lambda}_1$, and $\bar{\lambda}_2$ are selected as

$$\bar{\lambda}_i = \bar{\epsilon}^{(i-1)} \lambda_i^\star \qquad\qquad \bar{k}_i = \bar{\epsilon} k_i^\star \tag{9}$$

with $i = 1, 2$, and where $k_i^\star$ and $\lambda_i^\star$ are such that

$$\frac{\lambda_2^\star}{k_2^\star} < \frac{\lambda_1^\star}{4} \qquad 4 k_1^\star \lambda_1^\star < \frac{1}{m} \frac{\lambda_2^\star}{4} \qquad 6 \frac{k_1^\star}{k_2^\star} < \frac{1}{24} \frac{1}{m} \tag{10}$$

with $\bar{\epsilon} > 0$. The main properties of (2) driven by the control law (7)-(8) are summarised in the next proposition, whose proof has been omitted due to space limitations.

Proposition 1. Consider system (2) driven by the control law (7)-(8) in which $\bar{k}_i$ and $\bar{\lambda}_i$, $i = 1, 2$, have been selected according to (9) and (10), with $\bar{\epsilon} > 0$. Then, for all initial conditions $\left(\tilde{p}_e(t_0), \dot{\tilde{p}}_e(t_0)\right)$, we have that:

- $|\tau_q|_\infty \leq \sqrt{3} \bar{J} [mg + m |\ddot{p}_e^\star|_\infty + \bar{\epsilon} \lambda_2^\star$, with $\bar{J} = \max |J(q)|$.
- There exist $\bar{\Gamma}_1, \bar{\Gamma}_2 \in \mathbb{R}_{>0}$ such that

$$\left| \frac{\mathrm{d}\bar{\kappa}}{\mathrm{d}t} (\tilde{p}_e(t), \dot{\tilde{p}}_e(t)) \right|_\infty \leq \bar{\Gamma}_1 \bar{\epsilon}^2 + \bar{\Gamma}_2 \bar{\epsilon} |f_c|_\infty \tag{11}$$

- There exists $\Delta(\bar{\epsilon}) > 0$ and a class-$\mathcal{K}$ function $\gamma_{\bar{\epsilon}}$ such that, if $|f_c|_\infty \leq \Delta(\bar{\epsilon})$

$$|\tilde{p}_e|_a \leq \gamma_{\bar{\epsilon}} \left(|f_c|_a \right) \tag{12}$$

Despite the results in Prop. 1 only require the reference $p_e^\star(t)$ to be a sufficiently smooth function of time, additional constraints are introduced to support the stability results pertaining the aerial platform which are proposed in the next subsection. The scope is to bound the influence that the manipulator has on the position and attitude dynamics of the vehicle when tracking a reference $p_e^\star$.

Assumption 4.1. Let assume that for the trajectory $p_e^\star(t)$ there exist two constants $\bar{D}_2^\star$, $\bar{D}_3^\star \in \mathbb{R}_{>0}$ such that $|\ddot{p}_e^\star|_\infty \leq \bar{D}_2^\star$ and $\left| p_e^{\star,(3)} \right|_\infty \leq \bar{D}_3^\star$.

4.2 Modified thrust-vectoring control of the UAV

To stabilise the position of aerial platform to the constant references $p^\star$, the following *control vector* is defined

$$v_c = Mg\hat{e}_3 - \kappa(\tilde{p}, \dot{\tilde{p}}) \tag{13}$$

in which $\tilde{p} = p - p^\star$ is the position error, and $\kappa : \mathbb{R}^3 \times \mathbb{R}^3 \to \mathbb{R}^3$ is a feedback control law.

The control vector v_c is applied to the vehicle position dynamics (3) by properly *vectorizing* the thrust produced by the propeller. By taking advantage of the knowledge of the manipulator control inputs τ_q, a *control thrust* T_c and a *control attitude* θ_c are computed to have

$$R(\theta_c) \left[T_c \hat{e}_3' - J^{-\mathrm{T}}(q) \tau_q \right] = v_c \tag{14}$$

To compute a solution to (14), let us assume that, for all time $t \geq 0$, we have that $|v_c| > 0$, and

$$\left| T_c - \left[J^{-1}(q) \hat{e}_3' \right]^{\mathrm{T}} \tau_q \right| > 0 \tag{15}$$

The above assumptions are satisfied by properly tuning the position control laws of the manipulator and the UAV, see Prop. 3. From (14), we get that T_c is positive solution of

$$T_c^2 - 2 \left[J^{-1}(q) \hat{e}_3' \right]^{\mathrm{T}} \tau_q \, T_c + \tau_q^{\mathrm{T}} J^{-1}(q) J^{-\mathrm{T}}(q) \tau_q = v_c^{\mathrm{T}} v_c$$

provided that v_c is such that

$$v_c^{\mathrm{T}} v_c + \tau_q^{\mathrm{T}} J^{-1}(q) \left[\hat{e}_3' (\hat{e}_3')^{\mathrm{T}} - I \right] J^{-\mathrm{T}}(q) \tau_q > 0 \tag{16}$$

As far as the attitude θ_c is concerned, if $\hat{v}$ and $\hat{t}$ are the unitary vectors aligned with v_c and $T_c \hat{e}_3' - J^{-\mathrm{T}}(q) \tau_q$, respectively, we have that

$$R(\theta_c) = I + \mathcal{S}(w) + \frac{1 - c}{s^2} \mathcal{S}^2(w) \tag{17}$$

being $w = \hat{t} \times \hat{v}$, $s = |w|$ and $c = \hat{t}^{\mathrm{T}} \hat{v}$ the rotation axis, and the sine and cosine of the angle, respectively, that allow to align $\hat{t}$ with $\hat{v}$, and where $\mathcal{S}(\cdot)$ is the skew-symmetric cross-product matrix of a vector. While the control thrust T_c can be directly applied to the vehicle by choosing $T = T_c$, the control attitude θ_c is employed as a reference for the attitude stabilising control law.

To stabilize the position dynamics of the aerial vehicle, we focus on the following nested saturation control law

$$\kappa \left(\tilde{p}, \dot{\tilde{p}} \right) = \lambda_2 \sigma \left(\frac{k_2}{\lambda_2} \left(\dot{\tilde{p}} + \lambda_1 \sigma \left(\frac{k_1}{\lambda_1} \tilde{p} \right) \right) \right) \tag{18}$$

in which k_1, k_2, λ_1, and λ_2 are selected as

$$\lambda_i = \epsilon^{(i-1)} \lambda_i^\star \qquad\qquad k_i = \epsilon k_i^\star \tag{19}$$

with $i = 1, 2$, $\epsilon > 0$, and where $k_i^\star$, $\lambda_i^\star$ are the same of Prop. 1, and then such that (10) holds.

Proposition 2. Consider the control law (18) in which k_i and λ_i, $i = 1, 2$, have been selected according to (19) and (10), with $\epsilon > 0$. Then, for all the initial conditions $\left(\tilde{p}(t_0), \dot{\tilde{p}}(t_0)\right)$, and under assumption that $\left(q(t), p_e(t), p(t), \theta(t)\right) \in \Theta$, with Θ defined in (6), for all $t \geq 0$ (see Assumption 3.1), the following results hold true:

- $|\kappa(\tilde{p}, \dot{\tilde{p}})|_\infty \leq \sqrt{3} \lambda_2^\star \epsilon$.

- Let the reference $p_e^\star(t)$ satisfy Assumption 4.1. Then,
$$\left|\frac{\mathrm{d}\kappa}{\mathrm{d}t}(\tilde{p}(t),\dot{\tilde{p}}(t))\right|_\infty \leq \Gamma_{\bar{D}_2^\star}\epsilon \tag{20}$$
for some $\Gamma_{\bar{D}_2^\star} \in \mathbb{R}_{>0}$.
- The closed-loop dynamics $(\tilde{p}(t),\dot{\tilde{p}}(t))$ is ISS with restriction on the exogenous inputs τ_q and $\theta - \theta_c$.

This result shows how the position control input is bounded by a value that does not depend from the current position error, but only from the saturation parameters. This property, together with the analogous one for the manipulator proved in Prop. 1, is employed to analyse the behaviour of the overall closed-loop system in presence of contacts preventing the vehicle to maintain the desired lateral and vertical position asymptotically. Moreover, the ISS with restriction on the inputs property is instrumental for proving the ISS stability of the complete system.

Finally, the attitude control for the vehicle is designed. In particular, the control torque τ_c is defined as
$$\tau_c = \tau_{\mathrm{FF}}\left(\tau_q, q\right) + \tau_{\mathrm{FB}}\left(\theta, \dot{\theta}, \theta_c\right) \tag{21}$$
in which
$$\tau_{\mathrm{FF}}\left(\tau_q, q\right) = p_b' \times \left[J^{-\mathrm{T}}(q)\tau_q\right] \tag{22}$$
is the feed-forward control action compensating for the reaction torque produced by the manipulator, and
$$\tau_{\mathrm{FB}}\left(\theta, \dot{\theta}, \theta_c\right) = -k_P\left[(\theta - \theta_c) + k_D\dot{\theta}\right] \tag{23}$$
is the feedback stabilising control law. The stability of the system resulting from the interconnection with the robotic arm both in free-flight and in contact with the environment is discussed in the next proposition.

Proposition 3. Let us consider the system (3)-(4), in which the control inputs T and τ are selected as $T = T_c$ and $\tau = \tau_c$. Let the trajectory of the complete system be such that $\big(q(t), p_e(t), p(t), \theta(t)\big) \in \Theta$, with Θ defined in (6), for all $t \geq 0$ (see Assumption 3.1), the references $p_e^\star$ satisfy Assumption 4.1, and $\epsilon > 0$ be chosen such that
$$\sqrt{3}\lambda_2^\star\epsilon \leq Mg - \underline{v} \tag{24}$$
for some $mg < \underline{v} < Mg$, and let $|f_c|_\infty \leq \bar{F}$ for some $\bar{F} > 0$. Then, there exists $k_D^\star > 0$ and, for all $k_D < k_D^\star$, there exists positive $k_P^\star(k_D)$, $m^\star$ and $\bar{\epsilon}^\star$ with
$$\sqrt{6}\left[m^\star + m^\star\bar{D}_2^\star + \lambda_2^\star\bar{\epsilon}^\star\right] < \underline{v} \tag{25}$$
such that for all $k_P > k_P^\star$, $m < m^\star$, and $0 < \bar{\epsilon} < \bar{\epsilon}^\star$, there exists a $\Delta_0 > 0$ and a class-$\mathcal{K}$ function γ_p such that the closed-loop system is ISS with restriction Δ_0 on the initial conditions, restriction $\bar{F}$ on the exogenous input f_c, and
$$|\tilde{p}|_a \leq \gamma_p\left(\frac{k_D}{k_P}\left(\left|p_e^{\star,(3)}\right|_a + |f_c|_a\right)\right)$$

Proof. The proof is in Appendix A.

This is a local result (see e.g. Naldi et al. (2017) for a global one), and it shows how the aerial vehicle dynamics remain bounded in presence of the reaction forces applied by the manipulator. The effect of these disturbances can be arbitrarily reduced by increasing the gain of the attitude control loop. Note that the exogenous disturbance include also the unknown contact force f_c, thus showing the effectiveness of the proposed design in tasks requiring physical interaction. Hence, by considering also the result in Prop. 1 for the manipulator dynamics, the proposed control strategy achieves practical tracking of the desired references $(p^\star, p_e^\star(t))$ provided that the restrictions on the magnitude of the contact force f_c are satisfied. Moreover, when $f_c \equiv 0$, the tracking of the manipulator references becomes asymptotic and the UAV converges to the desired constant position, provided that $p_e^{\star,(3)}(t) \equiv 0$, i.e. the jerk of the reference end-effector trajectory is zero.

M	1.8 Kg
J_{uav}	diag (1.9, 1.9, 0.8) Kg · m^2
m	0.1 Kg
$(k_1^\star,\, k_2^\star)$	(1, 150)
$(\lambda_1^\star,\, \lambda_2^\star)$	(5, 150)
$(\epsilon,\, \bar{\epsilon})$	(0.1, 0.05)
$(k_P,\, k_D)$	(30, 9)

Table 1. Parameters of the setup.

5. EXPERIMENTAL RESULTS

The purpose of this section is to validate the theory presented in Section 4 by showing some experimental results. The aerial manipulator (see Fig. 1) consists of the ducted-fan prototype presented in Naldi and Marconi (2014) rigidly connected to the base plate of a parallel Delta robot, described in Keemink et al. (2012). The end-effector is an ultrasonic non-destructive testing sensor (see e.g. Hayward et al. (2006)) usually employed for inspection-by-contact of infrastructures. It is driven by 3 electric motors and it is characterized by a total weight lower than 150 gr. The workspace of the manipulator is approximately a sphere of 10 cm radius.

The prototype has been equipped with suitable avionics hardware. In particular, an Inertial Measurement Unit (IMU) is employed to obtain a high bandwidth (500 Hz) attitude information of the vehicle. On the other hand, the position of the ducted-fan is obtained by means of an OptiTrack motion tracking system capable of millimeter accuracy. Then, the position of the end-effector in the inertial frame can be then computed from the knowledge of the inertial position of the vehicle, and of the joint position of the manipulator thanks to the direct kinematic (5). The mechanical parameters of the system and the control parameters employed in the control laws (8), (18) and (23) are listed in Table 1.

The goal of the experiment is to show how the aerial vehicle can be stabilised to a constant position while the manipulator enters in contact with the environment. In Fig. 1, it is possible to observe the aerial robot performing a "docking manoeuvre," i.e. the robot enters in contact with a vertical surface, parallel to the $\hat{e}_3$ axis of the inertial reference frame, and at a certain position $\bar{x}$ along its path in the $\hat{e}_1$ direction. Due to space limitations, the experimental data only show the planar dynamics, i.e. the motion of the system in the $\hat{e}_1$ and $\hat{e}_3$ direction (here denoted by x and y), and the rotation θ around the $\hat{e}_1$ axis. In Fig. 2, the behaviour of the UAV during the two different phases that compose the experiment are presented. The first one, approximately from 70 s to 105 s, is denoted as the *Free Flight* phase since the vehicle is not in contact with the surface. The task is

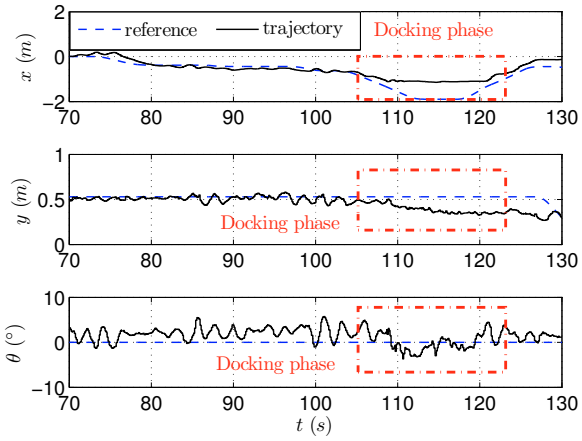

Fig. 2. Reference and trajectories in the x, y, and θ directions for the ducted fan UAV.

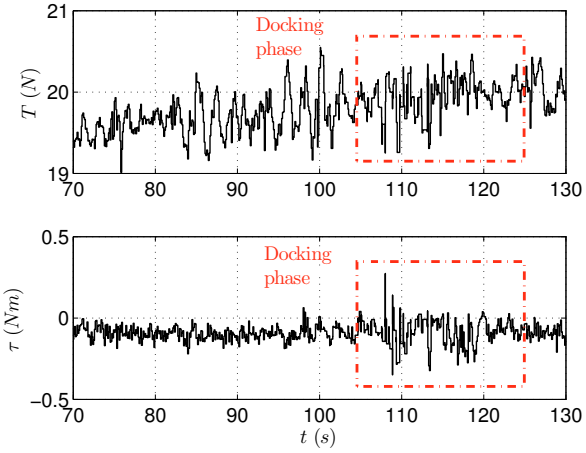

Fig. 3. The control input of the UAV: the thrust T and the torque τ applied around the $\hat{e}_1 \equiv \hat{e}'_1$ axis.

to track a longitudinal trajectory so as to stabilise a constant final desired position. The second phase, i.e. the *Docking / Contact* phase, starts after 105 s. Note, in fact, that the lateral position x that does not follow the "right" trajectory because of the obstacle. Furthermore, at the same time, the UAV tilts since the θ dynamics is directly influenced by the lateral error. The contact force also affects the vertical dynamics of the vehicle: in fact, a small tracking error can be also observed for the vertical position y. In summary, the aerial vehicle remains stable during the entire maneuver and, in the presence of the unknown contact forces, practical stability of the desired reference position is obtained.

In Fig. 3, the control inputs of the UAV, i.e. the thrust T and the torque τ have been reported. Note that, during the contact, the torque τ reaches higher values in order to stabilise the attitude dynamics. Finally, in the last picture (Fig. 4) the two contact forces f_y and f_x applied to the end effector of the robot manipulator are reported. It is interesting to observe that they are close to zero during the Free Flight maneuver (the mass of the end-effector is relatively small), and that they assume values different from zero during the docking phase.

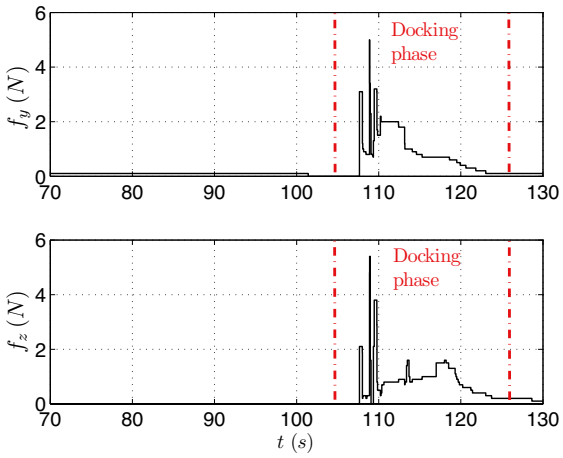

Fig. 4. The forces f_y and f_z applied to the end effector of the Delta manipulator.

6. CONCLUSIONS AND FUTURE ACTIVITIES

In this work, the control of a ducted-fan aerial robot equipped with a lightweight robotic arm and able to accomplish operations requiring the physical interaction with the surrounding environment is presented. Stability of the system both in the free flight and in the presence of contacts is achieved. The idea is to take into account explicitly of the reaction forces applied by the manipulator to the aerial platform so as to stabilize the vehicle to a constant desired position both in free-flight and during contacts. Interestingly enough, the proposed approach does not require an exact knowledge of the external force applied by the environment during interaction. Experiments, obtained with a ducted-fan aerial robot endowed with a Delta robotic arm, show how docking to a surface can be robustly achieved.

REFERENCES

Abdessameud, A. and Tayebi, A. (2010). Global trajectory tracking control of VTOL-UAVs without linear velocity measurements. *Automatica*, 46(4), 1053–1059.

Fumagalli, M., Naldi, R., Macchelli, A., Carloni, R., Stramigioli, S., and Marconi, L. (2012). Modeling and control of a flying robot for contact inspection. In *Intelligent Robots and Systems (IROS). Proceedings of the 2012 IEEE/RSJ International Conference on*, 3532–3537. Vilamoura, Portugal.

Hayward, G., Friedrich, M., and Galbraith, W. (2006). Autonomous mobile robots for ultrasonic NDE. In *IEEE Ultrasonics Symposium, Proceedings of the*, 902–906. Vancouver, Canada.

Hua, M., Hamel, T., Morin, P., and Samson, C. (2009). A control approach for thrust-propelled underactuated vehicles and its applications to VTOL drones. *Automatic Control, IEEE Transactions on*, 54(8), 1837–1853.

Isidori, A. (1999). *Nonlinear Control Systems II*. Communication and Control Engineering Series. Springer–Verlag.

Isidori, A., Marconi, L., and Serrani, A. (2003). *Robust Autonomous Guidance: An Internal Model Approach*. Advances in Industrial Control. Springer–Verlag, London.

Keemink, A., Fumagalli, M., Stramigioli, S., and Carloni, R. (2012). Mechanical design of a manipulation system for unmanned aerial vehicles. In *Robotics and Automation (ICRA). Proceedings of the 2012 IEEE International Conference on*. St. Paul, MN, USA.

Kobilarov, M. (2014). Nonlinear trajectory control of multi-body aerial manipulators. *Journal of Intelligent & Robotic Systems*, 73(1-4), 679–692.

Lippiello, V. and Ruggiero, F. (2012). Exploiting redundancy in cartesian impedance control of uavs equipped with a robotic arm. In *Intelligent Robots and Systems (IROS). Proceedings of the 2012 IEEE/RSJ International Conference on*, 3768–3773. Vilamoura, Portugal.

Marconi, L. and Naldi, R. (2007). Robust full degree-of-freedom tracking control of a helicopter. *Automatica*, 42(11), 1909–1920.

Marconi, L. and Naldi, R. (2012). Control of aerial robots. Hybrid force/position feedback for a ducted-fan. *Control Systems Magazine, IEEE*, 32(4), 43–65.

Marconi, L., Naldi, R., and Gentili, L. (2011). Modeling and control of a flying robot interacting with the environment. *Automatica*, 47(12), 2571–2583.

Mellinger, D., Shomin, M., Michael, N., and Kumar, V. (2013). *Distributed Autonomous Robotic Systems: The 10th International Symposium*, chapter Cooperative Grasping and Transport Using Multiple Quadrotors, 545–558. Springer, Berlin, Heidelberg.

Merlet, J.P. (2000). *Parallel Robots*. Kluwer Academic Publishers.

Naldi, R., Furci, M., Sanfelice, R., and Marconi, L. (2017). Robust global trajectory tracking for underactuated VTOL aerial vehicles using inner-outer loop control paradigms. *Automatic Control, IEEE Transactions on*, 62(1), 97–112.

Naldi, R., Gentili, L., Marconi, L., and Sala, A. (2010). Design and experimental validation of a nonlinear control law for a ducted-fan miniature aerial vehicle. *Control Engineering Practice*, 18(7), 747–760.

Naldi, R. and Marconi, L. (2014). A prototype of ducted-fan aerial robot with redundant control surfaces. *Journal of Intelligent & Robotic Systems*, 76(1), 137–150.

Appendix A. PROOF OF PROPOSITION 3

First of all, note that (24), (25) and $\bar{\epsilon} < \bar{\epsilon}^\star$ ensure that (15) and (16) are satisfied. Given the position dynamics of the UAV (3), the control law (18), and the change of coordinates $\zeta_1 = \tilde{p}$ and $\zeta_2 = \dot{\tilde{p}} + \lambda_1 \sigma\left(\frac{k_1}{\lambda_1}\zeta_1\right)$, the position error dynamics can be written as

$$\begin{aligned} \dot{\zeta}_1 &= -\lambda_1 \sigma\left(\frac{k_1}{\lambda_1}\zeta_1\right) + \zeta_2 \\ M\dot{\zeta}_2 &= -\lambda_2 \sigma\left(\frac{k_2}{\lambda_2}\zeta_2\right) + M k_1 \sigma'\left(\frac{k_1}{\lambda_2}\zeta_1\right)\dot{\zeta}_1 + \Gamma_\eta(\eta_1, \tau_q) \end{aligned} \tag{A.1}$$

where $\Gamma_\eta(\eta_1, \tau_q) = [R(\theta) - R(\theta_c)]\left[T_c \hat{e}_3' - J^{-\mathrm{T}}(q)\tau_q\right]$ is the auxiliary input, being $\eta_1 = \theta - \theta_c$. Note that $\Gamma_\eta(0, \tau_q) = 0$ for all $\tau_q \in \mathbb{R}^3$, and for all $\eta_1 \in \mathbb{R}^3$ we have that $|\Gamma_\eta(\eta_1, \tau_q)|_\infty \leq \bar{\Gamma}_{\eta,1}|\tau_q|_\infty + \bar{\Gamma}_{\eta,2}$ for some positive constants $\Gamma_{\eta,1}$ and $\Gamma_{\eta,2}$. In the new coordinates, we have that $\kappa(\zeta_1, \zeta_2) = \lambda_2 \sigma\left(\frac{k_2}{\lambda_2}\zeta_2\right)$, which implies that

$$\begin{aligned} \frac{\mathrm{d}\kappa}{\mathrm{d}t}(\zeta_1(t), \zeta_2(t)) = \frac{k_2}{M}\sigma'\left(\frac{k_2}{\lambda_2}\zeta_2\right)\Bigg[\lambda_2 \sigma\left(\frac{k_2}{\lambda_2}\zeta_2\right) + \\ + M k_1 \sigma'\left(\frac{k_1}{\lambda_1}\zeta_1\right)\dot{\zeta}_1 + \Gamma_\eta(\eta_1, \tau_q)\Bigg] \end{aligned} \tag{A.2}$$

From (Isidori et al., 2003, Appendix C), it is possible to prove that (A.1) is ISS with non-zero restrictions on the input Γ_η. Moreover, thanks to the change of coordinates $\eta_1 = \theta - \theta_c$ and $\eta_2 = \dot{\theta} + \frac{\eta_1}{k_D}$ the closed-loop attitude error dynamics can be written as

$$\begin{aligned} \dot{\eta}_1 &= -\frac{\eta_1}{k_D} + \eta_2 - \dot{\theta}_c \\ J_{\mathrm{uav}}\Omega(\eta_1 + \theta_c)\dot{\eta}_2 &= -\omega \times J_{\mathrm{uav}}\omega - k_P k_D \eta_2 + \\ &\quad + J_{\mathrm{uav}}\left[\frac{1}{k_D} + \dot{\Omega}(\eta_1 + \theta_c)\right]\cdot \\ &\quad \cdot\left(\eta_2 - \frac{\eta_1}{k_D}\right) + \frac{J_{\mathrm{uav}}}{k_D}\dot{\theta}_c \end{aligned} \tag{A.3}$$

in which we have that $\omega = \Omega(\theta)\dot{\theta} = \Omega(\eta_1 + \theta_c)\left(\eta_2 - \frac{\eta_1}{k_D}\right)$, with $\Omega(\theta)$ introduced in (4). Note that (17) implies that both θ_c and $\dot{\theta}_c$ are some bounded functions of v_c, $\dot{v}_c$, τ_q and $\dot{\tau}_q$. From (7) and (13) we get that τ_q and v_c are bounded by construction, while from (13), we have that $\dot{v}_c = -\dot{\kappa}(\tilde{p}, \dot{\tilde{p}})$, with $\dot{\kappa}$ computed in (A.2). From (7), we can also write that

$$\begin{aligned} \dot{\tau}_q = J^{\mathrm{T}}(q)R^{\mathrm{T}}(\theta)\left[m p_e^{\star,(3)} - \frac{\mathrm{d}}{\mathrm{d}t}\bar{\kappa}(\tilde{p}_e, \dot{\tilde{p}}_e)\right] + \\ + \left\{\frac{\mathrm{d}}{\mathrm{d}t}\left[J^{\mathrm{T}}(q)R^{\mathrm{T}}(\theta)\right]\right\}\left[m\left(\ddot{p}_e^\star + g\hat{e}_3\right) - \bar{\kappa}(\tilde{p}_e, \dot{\tilde{p}}_e)\right] \end{aligned}$$

and then by Prop. 2 that

$$\begin{aligned} |\dot{\tau}_q| \leq \lambda_1^e[m(D_2^\star + g) + \bar{\epsilon}]\left(|\eta_2| + \frac{|\eta_1|}{k_D}\right) + \\ + \bar{J}\left[|p_e^{\star(3)}| + |\dot{\bar{\kappa}}(\tilde{p}_e, \dot{\tilde{p}}_e)|\right] \end{aligned}$$

for some positive λ_1^e.

The closed-loop dynamics of the UAV results from the feedback interconnection of (A.1) and (A.3). Due to space limitations this part of the proof is only sketched. By considering an ISS-Lyapunov function $V(\eta_1, \eta_2) = \frac{1}{2}\eta_1^{\mathrm{T}}\eta_1 + \frac{1}{2}\eta_2^{\mathrm{T}}\Omega^{\mathrm{T}}(\eta_1)J_{\mathrm{uav}}\Omega(\eta_1)\eta_2$, and choosing k_D and k_P sufficiently small and large, respectively, and for m and $\bar{\epsilon}$ sufficiently small, system (A.3) can be shown to be ISS with respect to the exogenous input $\dot{v}_c = -\dot{\kappa}(\tilde{p}, \dot{\tilde{p}})$, $p_e^{\star,(3)}$, and $\dot{\bar{\kappa}}(\tilde{p}_e, \dot{\tilde{p}}_e)$, with an arbitrary asymptotic gain. From Propositions 1 and 2, and from the fact that $|f_c|_\infty$ is bounded, it is clear that $\dot{\kappa}$ and $\dot{\bar{\kappa}}$ are also bounded. Moreover, according to Assumption 4.1, also $p_e^{\star,(3)}$ is bounded. Then, it is possible to choose k_D and k_P to satisfy the restrictions on the input (see Prop. 2) on the position error subsystem (A.1) in finite time, and then to enforce the small gain condition. The final result is a consequence of standard ISS arguments, as in (Isidori et al., 2003, Appendix C).